Distance Distribution Analysis of Small-Angle X-ray Scattering for Semidilute Polyelectrolyte Solutions without Salts

Keisuke Kaji,* Hiroshi Urakawa, Toshiji Kanaya, and Ryozo Kitamaru

Institute for Chemical Research, Kyoto University, Uji, Kyoto-Fu 611, Japan.
Received July 18, 1983

ABSTRACT: The small-angle X-ray scatterings for semidilute solutions of poly(vinyl hydrogen sulfate) (PVSH) and its Li^+, Na^+, and K^+ metallic salts in the absence of added salts are analyzed in terms of an electron density distance distribution. Two peaks in regard to intra- and intersegmental correlation are observed in the distance distribution function that has been obtained by inverse Fourier transform of small-angle X-ray scattering intensity. The intrasegmental correlation increases in intensity with the number of electrons of the counterion. This directly evidences the condensation of counterions on the polyion. In relation to intersegmental correlation only a single peak is detected; the correlation distances are 88–101 Å for PVSH and its salts in a concentration of 0.2 monomer mol/L. No longer correlation peaks are observed. This suggests that only the nearest-neighbor intersegmental correlation exists in the semidilute solution. The maximum position of the intersegmental correlation somewhat depends on the kind of counterion. This may be explained by inhomogeneous counterion condensation on the polyion.

1. Introduction

The structure of semidilute polyelectrolyte solutions is one of the recent active problems. Scattering experiments using small-angle neutrons or X-rays provide useful information on this problem and several studies have been carried out[1-3] in which it was shown that the small-angle scattering gives a single broad peak. The peak may be interpreted in terms of correlation holes which are caused by the Coulombic repulsion between polyions. From this point of view, de Gennes et al.[4] introduced a scaling theory and, thereafter, Odijk[5] improved this theory to formulate possible scaling relations extensively.[6,16] These scaling relations, in the absence of salts, predict characteristic features of the scattering curves $S(q)$, where q is the magnitude of the scattering vector, namely, (i) that the concentration dependence of the maximum position q_m varies as $q_m \propto c^{1/2}$, (ii) that $S(q)$ varies linearly with q for $q < q_m$, and (iii) that $S(q) \sim q^{-1}$ for $q \gg q_m$. These relations have been confirmed for individual q ranges by neutron scattering experiments.[3] We have also confirmed the last two relations using X-ray scattering in the present study. However, we do not discuss the scaling relations in detail but use them only to remove the effect of interparticle interferences roughly and to estimate more correct cross-sectional sizes of polyions.

In this work we have studied salt-free semidilute polyelectrolyte solutions from different points of view. In spite of recent reports[1-3,7,8] favoring the isotropic model proposed by de Gennes et al.,[4] the diffraction peak sometimes tempts one to consider a lattice model,[9,10] in which extended polyion sections are arranged parallel. Therefore, we believe it is desirable to show clearly that no lattice regions exist in the solution. Distance distribution analysis[11] is one of the best methods for this purpose. For the isotropic model, the distance distribution function will show a sufficiently strong nearest-neighbor correlation peak, compared with second or higher neighbor one. On the other hand, the lattice model will give several strong correlation peaks at distances corresponding to near integral multiples of a lattice translation.

In addition to this point, the analysis is also useful to examine the counterion localization around polyions since intra- and intersegmental correlations are roughly separable when deep correlation holes exist in the system. The problem of ion binding has been studied in a number of papers, which are classified into two different approaches. One approach is based on the Poisson–Boltzmann equation[12,13] and the other based on the condensation theory by Oosawa[14] and Manning.[15] Although these two approaches are involved in a controversy,[16] they afford essentially the same result for polyelectrolytes with high charge density as in the present study, where a part of the counterions are strongly bound on polyions.[17,18] The effect of dielectric saturation on the counterion concentration around the polyion was also examined by Troll and Zimm[19] and it was found that it is negligibly small. In this work, we show from intrasegmental correlations and the cross-sectional area of polyion that a considerable amount of counterions is strongly bound on polyions.

2. Experimental Section

2.1. Samples. The commercially available potassium salt of poly(vinyl hydrogen sulfate) $[-CH_2CH(OSO_3H)-]_n$ with an average degree of polymerization $\bar{p} \approx 1500$ and a degree of esterification $\alpha = 96.1\%$ was purified by deionization using anion- and cation-exchange resins (Amberlite IR120B and IRA400, respectively). The resulting poly(vinyl hydrogen sulfate) (PVSH) was completely neutralized with various alkalis such as LiOH, NaOH, and KOH by coulometric titration and then lyophilized. The concentration of the polyelectrolyte aqueous solutions used for the scattering measurements was 0.2 monomer mol/L in all cases. In the case of solutions of metallic salts no hydrolysis occurred even after 2 months, which was checked by precipitating free sulfuric groups with barium ions. On the other hand, the acid form of the polyelectrolyte was easily hydrolyzed. Accordingly, scattering measurements were carried out immediately after preparation of the solution.

2.2. Small-Angle X-ray Scattering (SAXS) Measurements. SAXS intensities were measured by using a block camera,[20] a Kratky compact camera (Anton Paar K. G. KCEC) with a proportional counter. Ni-filtered and pulse-height-analyzed Cu Kα radiation generated at 40 kV and 45 mA was used. In order to avoid fluctuation of the source intensity the temperature of cooling water (deionized) for the X-ray tube target was controlled to be 19 ± 0.2 °C, and the room temperature was kept within 20 ± 0.5 °C. The resulting source intensity was held constant within 0.3%. The sample-to-detector distance was 200 mm, and the widths of incoming and receiving line slits were chosen as 100 and 250 μm, respectively. A fixed-time counting technique was employed; the intensity was counted for 1000 s at each scattering position. The width of the scanning step was changed to 100, 200, 500, and 1000 μm corresponding to four scattering ranges. The observed intensity from solutions was corrected for sample absorption,[21] and then the scattering intensity of water was subtracted. The correction for the length and width of the beam was made by using a new method developed by the present authors,[22] in which the curve is fitted with three-order B-spline functions smeared by the slit geometry and the accuracy of fitting is judged by AIC (Akaike's information criterion).[23] Thus the observed curve is desmeared unequivocally. The scattering curves desmeared by

0024-9297/84/2217-1835$01.50/0

this new method essentially agree with those by Glatter's method[24] but are somewhat different in the low q range.

2.3. Distance Distribution Analysis. The correlation obtained by the inverse Fourier transform of scattering intensity is the average of the product of two electron density fluctuations at a distance r. The correlation function is therefore defined as

$$\gamma(r) = \langle \eta(\vec{r}_1)\eta(\vec{r}_2) \rangle \quad (1)$$

where $r = |\vec{r}_1 - \vec{r}_2|$ and $\eta(\vec{r}) = \rho(\vec{r}) - \bar{\rho}$, $\rho(\vec{r})$ being the electron density at $\vec{r}$, and $\bar{\rho}$ the average in the whole system. Further, the distance distribution function defined as

$$P(r) = 4\pi r^2 \gamma(r) \quad (2)$$

is proportional to the number of pairs of difference electrons separated by the distance r.

The function $P(r)$ is given by Fourier inversion of the scattering intensity $i(q)$

$$P(r) = \frac{2}{\pi} \int_0^\infty rqi(q) \sin(rq)\, dq \quad (3)$$

where $q = 4\pi(\sin\theta)/\lambda$, 2θ is the scattering angle, and λ the X-ray wavelength. The scattering intensity $i(q)$ is experimentally obtained from the relation

$$i(q) = I_s(q) - I_0(q) \quad (4)$$

where $I_s(q)$ and $I_0(q)$ designate scattering intensities of the polyelectrolyte solution and pure water, respectively. In the present experiments, $i(q)$ was observed over the range $0.02 < q < 0.45$ Å^{-1}, corresponding to 300–14 Å in distance, and the intensities at the lower and upper limits of q were not zero. To calculate $P(r)$ from the observed scattering intensity $i(q)$ using eq 3, it is necessary to extrapolate the observed $i(q)$ from $q = 0$ to $q = \infty$. The extrapolation $q \to 0$ is not very difficult and it hardly affects calculated results in a distance range 0–300 Å, independently of different extrapolations. However, the reasonable extrapolation $q \to \infty$ is problematic since generally we do not know the true shapes of scattering curves over a wide q range. To avoid such a difficulty, a damping factor is usually employed because it is well-known that the damping factor is an artificial temperature factor and does not affect peak positions in the distance distribution function, although peak intensities are somewhat reduced. Thus, for the present calculations of $P(r)$ the modified intensity was used instead of $i(q)$

$$i'(q) = i(q) \exp(-Dq^2) \quad (5)$$

where D is the damping coefficient. To remove the truncation effect, D had to be taken as 20.0 Å^2, but it is not very large since it corresponds to a fluctuation of 4.5 Å around the average position. As this is the first application of distance distribution analysis to polyelectrolyte solutions, we have checked the validity of the damping factor. The functions $P(r)$ have been calculated for some possible extrapolated scattering curves. In the high q range, polymer chains in the solution may be regarded as rods or spheres (blobs in a scaling concept[26]) in two extreme cases. The scattering functions in the high q range for a rod and a sphere are proportional to q^{-1} and q^{-4} (Porod's rule), respectively.[11,25] The scattering functions for intermediate conformations may therefore be assumed proportional to q^{-n} ($1 \le n \le 4$). We calculated $P(r)$'s for the scattering curves extrapolated according to the q^{-n} law with n = 1, 2, 3, and 4. In the practical calculations $i(q)$ was extrapolated to $q = 8.29$ Å^{-1}, where the intensity was negligibly small. As an example, the results for PVSK are shown in Figure 1. Curves a–d correspond to the cases with n = 1–4 and curve e is the result calculated by using the damped intensity function eq 5. As seen from the figure, the obtained functions $P(r)$ agree well with one another. This shows that the different extrapolations hardly affect the calculated results. Small ripples in cases c and d are, however, due to the nonsmooth connections when the scattering curves are extrapolated. This shows that one cannot extrapolate $i(q)$ according to the q^{-3} or q^{-4} law. Extrapolations according to q^{-1} and q^{-2} law give almost the same results, which agree well with that from the damped scattering curve e except for a slight difference of intensity for the first peaks in $P(r)$. The slightly lower intensity for (e) comes from the damping factor used since the factor lowers the scattering intensity more intensely in the higher q range. It should therefore be noticed that when the scattering curve was damped, the calculated intensity of $P(r)$ is underestimated more for shorter distances though the amount is small. From this point of view the $P(r)$ function calculated from the q^{-1} or q^{-2} extrapolation is closer to the true one. Moreover, the q^{-1} law is supported from the scaling law.[3] However, in this study we use eq 5 since we do not know whether the q^{-1} law is exactly valid in every case. For an example, the tail of the small-angle scattering curve is often affected by wide-angle scatterings[27] as will be shown later. The damping factor reduces such an effect.

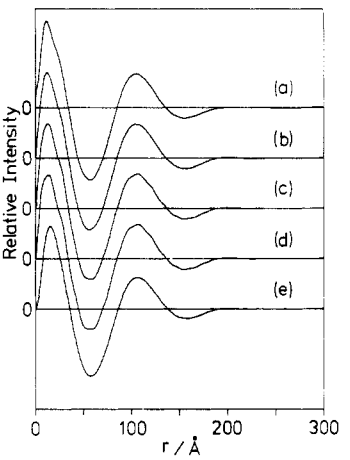

Figure 1. Distance distribution functions for a semidilute solution of potassium salt of poly(vinyl hydrogen sulfate). Curves a, b, c, and d are results for the scattering curves extrapolated according to q^{-n} law with n = 1, 2, 3, and 4, respectively. Curve e is a result for the damped scattering curve.

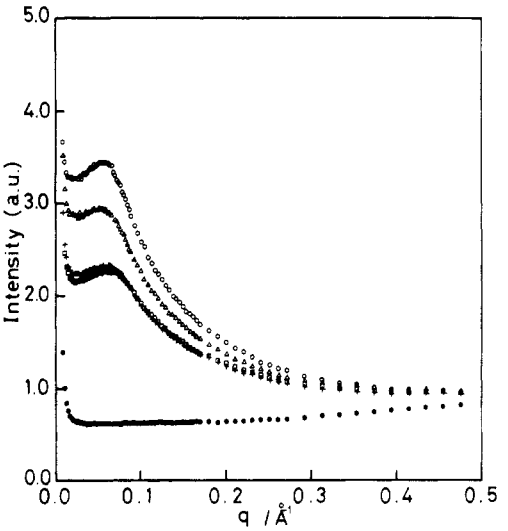

Figure 2. Observed small-angle X-ray scattering (SAXS) curves of semidilute solutions of poly(vinyl hydrogen sulfate) (PVSH) and its lithium, sodium, and potassium salts (PVSLi, PVSNa, PVSK). Concentration is 0.2 monomer mol/L in every case, average degree of polymerization $\bar{p} \approx 1500$, and degree of esterification α = 96.1%. PVSH (□), PVSLi (+), PVSNa (▲), PVSK (○), water (●).

3. Results

Figure 2 shows the observed SAXS curves of semidilute aqueous solutions of poly(vinyl hydrogen sulfate) (PVSH) and its metallic salts after correcting for absorption. Li, Na, and K salts are designated by PVSLi, PVSNa, and PVSK, respectively. The lowest curve is the scattering of pure water. It is seen that each curve for the solutions exhibits a broad peak at q_m = 0.055–0.065 Å^{-1}. The scattering curves which were desmeared after subtraction of the scattering of pure water are shown in Figure 3. The peaks become sharper and the maximum positions shift

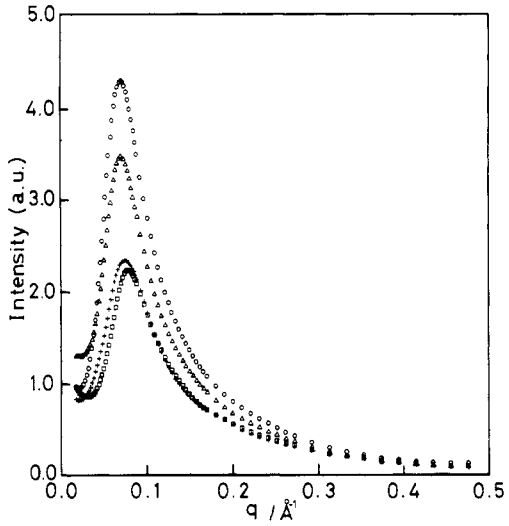

Figure 3. Corrected SAXS curves of Figure 2. PVSH (□), PVSLi (+), PVSNa (△), PVSK (○).

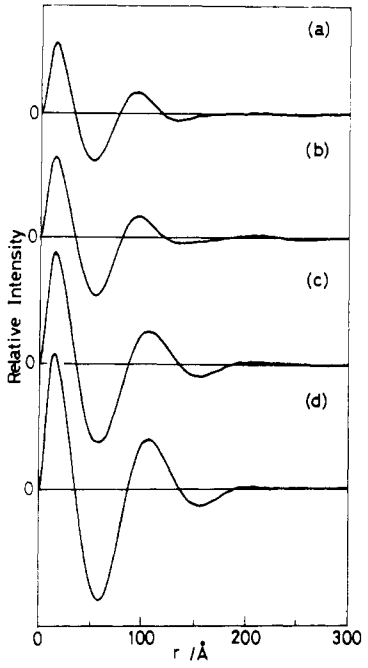

Figure 4. Distance distribution functions of semidilute solutions of poly(vinyl hydrogen sulfate) and its metallic salts. (a) PVSH, (b) PVSLi, (c) PVSNa, (d) PVSK.

slightly (by ca. 0.005 $Å^{-1}$) in the direction of higher q in all cases. The scattering of PVSH corresponds to that of polyions without counterions since protons H^+ do not contribute to the scattering. The effect of the kind of counterions on the scattering is evident in Figure 3. The peak intensity greatly increases with the number of electrons in the counterion: 2, 10, and 18 for Li^+, Na^+, and K^+. It is also noticed that the peak positions are different depending on the kinds of counterions, though the difference is very small, e.g., 0.005 $Å^{-1}$.

The distance distribution function $P(r)$, which is defined by eq 2, has been calculated for PVSH and its metallic salts. The results are shown in Figure 4. The line $P(r) = 0$ corresponds to the average distance distribution density over the total solution system. As seen from the figure, all $P(r)$ functions have two peaks in the range 0–300 Å; the first peak is considered to be related to intrasegmental correlation. The maximum position of this peak, however, does not mean any characteristic correlation length since $P(r)$ is deformed due to a factor of $4\pi r^2$ from the correlation function $\gamma(r)$ which has its maximum intensity at $r = 0$. The second peak is related to intersegmental correlation since a deep correlation hole is seen between the first and second peaks. It is noticed here that no further peak can be observed in addition to the two peaks cited about. This suggests that only the nearest-neighbor intersegmental correlation exists in the semidilute solution of salt-free polyelectrolyte.

Table I
Some Characteristic Parameters of Semidilute Solutions of Poly(vinyl hydrogen sulfate) (PVSH) and Its Lithium, Sodium, and Potassium Salts (PVSLi, PVSNa, and PVSK)[a]

polyelectrolyte	ξ^b/Å	r_0^c/Å	$(\Delta\rho)^2/(\Delta\rho)^2_{PVSH}$[d] from $\gamma(0)$	$(\Delta\rho)^2/(\Delta\rho)^2_{PVSH}$[d] from slope of eq 8
PVSH	88	5.1 ± 0.3	1.00	1.00
PVSLi	90	5.2 ± 0.3	1.00	1.02
PVSNa	100	5.9 ± 0.4	1.30	1.45
PVSK	101	6.1 ± 0.4	1.57	1.67

[a] The concentration is 0.2 monomer mol/L in every case, the average degree of polymerization $\bar{p} \approx 1500$, and the degree of esterification $\alpha = 96.1\%$. [b] Intersegmental correlation length. Estimation error is less than 1%. [c] Radius of polyion cross section. [d] Ratio of square excess density.

To discuss correlation lengths quantitatively, $\gamma(r)$ has been calculated from $P(r)$ because the peak positions in $P(r)$ do not give correct correlation lengths owing to a weighting factor of $4\pi r^2$. Although the calculated curves are not shown here, two correlation peaks corresponding to those in $P(r)$ are also seen in $\gamma(r)$. The peak intensity of intrasegmental correlation at $r = 0$ is more than 100 times higher than that due to intersegmental correlation. Intersegmental correlation lengths, which here mean distances corresponding to the maximum intensity of intersegmental correlation, are summarized in Table I. The $\gamma(r)$ function of PVSH represents the correlation regarding pure polyion without counterions; its intersegmental correlation length is 88 Å. The effect of the type of counterion was examined next. In the case of Li^+ the intensity of the first intrasegmental peak becomes a little stronger as is also shown from $P(r)$ (Figure 4b), and the second intersegmental peak position increases slightly to 90 Å. The weak effect comes from the fact that Li^+ has only two electrons. In the cases of Na^+ and K^+, however, the correlation intensity of difference electrons increases remarkably in both the first and second correlation peaks and the maximum position of the second peak shifts to 100–101 Å. The increase in intensity of the intra- and intersegmental correlation peaks is direct evidence that a considerable amount of counterions is condensed on the polyions. The remaining counterions are considered to be distributed homogeneously in the solution. If they were localized somewhere, e.g., between polyion segments, a corresponding correlation peak would be observed between the first and second peaks in $\gamma(r)$ or $P(r)$. However, no such peak is observed as seen from Figure 4c,d.

4. Discussion

As described in the Introduction, every scattering curve $S(q)$ observed in the present study (Figure 3) fits the scaling relations[3] $S(q) \sim q$ for $q < q_m$ and $S(q) \sim q^{-1}$ for $q \gg q_m$. The latter relation is, however, valid only for $0.2 < q/Å^{-1} < 0.35$ as will be shown later; departures for $q > 0.35$ $Å^{-1}$ may be due to the superposition of the tail of wide-angle scattering.[27] We do not discuss the scaling relations here in any further detail.

One of the most interesting problems is the structure of a semidilute salt-free polyelectrolyte solution. The

distance distribution function $P(r)$ analyzed in this work showed only one single intersegmental correlation peak. This strongly supports the isotropic model proposed by de Gennes[4] because in this model nearest-neighbor correlations are presumed predominant. The single intersegmental peak also shows that the lattice model is incorrect, since if the model is right, several strong intersegmental correlation peaks at distances corresponding to near integral multiples of a lattice translation would be seen in the function $P(r)$. Further, the function $P(r)$ consists of intra- and intersegmental components $P_1(r)$ and $P_2(r)$ and subtraction of $P_1(r)$ from $P(r)$ gives $P_2(r)$, which we discuss qualitatively below. As has already been pointed out, the first and second peaks in $P(r)$ are mainly related to intra- and intersegmental correlations, respectively. If we assume that the first peak is solely $P_1(r)$ as a first approximation, we can calculate $P_2(r)$. Judging from the fact that a large negative minimum exists between the first and the second peaks in $P(r)$, we may consider that $P_2(r)$ has a deep negative hole in the distance range 0 to 70 or 80 Å. This shows that the intersegmental interaction is repulsive, which agrees with the result of small-angle neutron scattering by Williams et al.[1] One more important point to be noted is that no peak is present at about half of the intersegmental correlation distance (40–50 Å). This means that uncondensed counterions are not localized between correlating segments; they are probably distributed homogeneously in the solution. This again does not agree with the lattice model since the model is often stabilized by localizing counterions in the middle position between parallel segments.[10]

A further problem is counterion condensation. According to the condensation theory,[14,15] more than 65% of the total counterions are expected to condense on the polyion in the present system because the ratio of electrostatic to kinetic energy for PVSH is about 3. Such an expectation is qualitatively confirmed in the present experiment. It is presumed that the effect of counterion condensation on the polyion appears directly in the intensity at $r = 0$ of the correlation function $\gamma(r)$; the intensity will increase with the increasing number of electrons of the counterion. The function $\gamma(r)$ is easily calculated from eq 2 on an arbitrary scale, and the ratio of $\gamma(0)$, for various counterions, to that of PVSH is listed in Table I. The function $\gamma(0)$ increases with the increasing number of electrons on the counterion, which supports the concept of counterion condensation. At the present stage, however, quantitative estimation of the number of condensed counterions is difficult since absolute scattering intensity measurements are necessary. One more consequence of counterion condensation is the increase of the cross section of a polyion. To confirm this, the radii of cross section for the pure and the counterion condensed polyions have been determined.

In a dilute system of rods with diameter $2r_0$, length l and an excess electron density $\Delta\rho$, the intensity function is approximately given by

$$S_0(q) \approx k(\Delta\rho)^2 \exp(-q^2r_0^2/4)/ql \qquad (6)$$

for $2l^{-1} \ll q < r_0^{-1}$ where k is a constant.[28] In a concentrated system, however, eq 6 is no longer valid because of interparticle interference, so that r_0 cannot be obtained directly from this equation. According to the scaling concept, the intensity function for a concentrated system is described by

$$S(q) = S_0(q)\frac{q^2\xi^2}{1 + q^2\xi^2} \qquad (7)$$

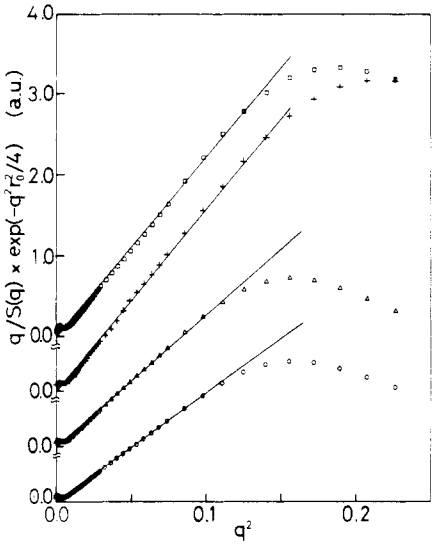

Figure 5. Plot of $q \exp(-r_0^2q^2/4)/S(q)$ vs. q^2 for semidilute solutions of poly(vinyl hydrogen sulfate) and its metallic salts. PVSH (□), PVSLi (+), PVSNa (△), PVSK (○).

where ξ is the average distance between neighboring chains. Using this equation, we remove the interparticle interferences roughly and estimate a more accurate radius of cross section than that obtained without using eq 7. Combining eq 6 and 7, we obtain for $2b^{-1} \ll q < r_0^{-1}$

$$\frac{q}{S(q)} \exp\left(-\frac{r_0^2}{4}q^2\right) = \frac{b}{k(\Delta\rho)^2\xi^2}(\xi^2q^2 + 1) \qquad (8)$$

where b is the persistence length. The plot of $q \exp(-r_0^2q^2/4)/S(q)$ vs. q^2 will give a straight line within the above q range when r_0 has been the correct value. Such plots for PVSH, PVSLi, PVSNa, and PVSK are shown in Figure 5. In all cases the observed values fit closely to a straight line going through the origin within a q range of 0.08–0.4 Å^{-1}. Because of large ξ, it is reasonable that the intercept of the straight line is negligibly small in the scale of Figure 5. Departures from the linearity in the high q range may be due to the superposition of the tail of wide-angle scattering.[27] The most suitable values of r_0 and the excess densities of the solutions calculated from the slope of the straight line in Figure 5 are also listed in Table I. As was presumed, the radius of cross section of the polyion increases with the number of electrons on the counterion. The difference of r_0 between PVSH and PVSK is about 1 Å, which is comparable to the radius of the counterion K^+ (1.35 Å).[29] This is strong support for a considerable amount of counterions being condensed on the polyion. Further, the increase of excess density with increasing counterion size also favors the above concept.

In conclusion we discuss the dependence of the intersegmental correlation distance on the kind of counterion, e.g., 88 and 101 Å for PVSH and PVSK, respectively. One possible explanation is an inhomogeneous counterion condensation. As was already described, in the polyelectrolyte solutions under discussion only nearest-neighbor correlations among intersegments exist. Therefore, the intersegmental correlation distance is affected by the counterion distribution about the polyion chain axis. If the condensed counterions are localized more on the outer sides of a pair of nearest-neighbor segments, the observed result may be explained since the larger counterions contribute more strongly to the correlations and increase the correlation distance. This is possible because between the segments electrostatic repulsive forces interact arising from unsaturated negative charges on the polyion. Such re-

pulsive forces make the anion side groups orient more strongly to the outer sides and increase the charge density of the outer side. The larger charge density then condenses more counterions. If the segments are extended, anionic side groups of poly(vinyl hydrogen sulfate) orient to one side of the plane perpendicular to the planar zigzag plane of the carbon skeleton. In such a case it is energetically more stable that the anionic side groups orient to the opposite sides. Such a tendency may occur in practice. The above discussion does not contradict the increase of polyion cross section. The difference of the intersegmental correlation distances can be roughly estimated from the radii of cross section of polyions. For example the difference between PVSH and PVSK is calculated to be about 12–14 Å, which agrees with the observed value of 13 Å.

The possibility that the intersegmental correlation distance increases with increasing radius of cross section of a homogeneous polyion cylinder may be excluded, although we have not confirmed this by calculating correlation functions $\gamma(r)$. The $\gamma(r)$ function consists of intra- and intersegmental components; the former component decreases monotonically from the maximum intensity at $r = 0$ to zero with increasing r. On the other hand, the latter component increases from zero to a maximum intensity and then goes through a shallow minimum to approach the average intensity of the system. With increasing size of cross section of the cylinder, intra- and intersegmental peaks in $\gamma(r)$ become broader in width but the peak positions do not change. If the tail of the intersegmental correlation peak is superposed on the intersegmental peak, the latter peak position should shift to a shorter distance because the tail of the intrasegmental curve has a negative slope. However, the observed results are the opposite.

Acknowledgment. We are indebted to Emeritus Professor Ichiro Sakurada of Kyoto University for his fruitful discussions and suggestions and to Dr. Masao Hosono for his helpful suggestions for sample preparations and discussions.

Registry No. PVSH, 26101-52-0; PVSLi, 27940-33-6; PVSNa, 25053-27-4; PVSK, 27940-34-7.

References and Notes

(1) Williams, C. E.; Nierlich, M.; Cotton, J. P.; Jannink, G.; Boué, F.; Daoud, M.; Farnoux, B.; Picot, C.; de Gennes, P.-G.; Rinaudo, M.; Moan, M.; Wolff, C. *J. Polym. Sci., Polym. Lett. Ed.* **1979**, *17*, 379.
(2) Nierlich, M.; Williams, C. E.; Boué, F.; Cotton, J. B.; Daoud, M.; Farnoux, B.; Jannink, G.; Picot, C.; Moan, M.; Wolff, C.; Rinaudo, M.; de Gennes, P.-G. *J. Phys. (Orsay, Fr.)* **1979**, *40*, 701.
(3) Hayter, J.; Jannink, G.; Brochard-Wyart, F.; de Gennes, P.-G. *J. Phys. Lett. (Orsay, Fr.)* **1980**, *41*, L-451.
(4) de Gennes, P.-G.; Pincus, P.; Velasco, R. M.; Brochard, F. *J. Phys. (Orsay, Fr.)* **1976**, *37*, 1461.
(5) Odijk, T. *J. Polym. Sci. Polym. Phys. Ed.* **1977**, *15*, 477.
(6) Odijk, T. *Macromolecules* **1979**, *12*, 688.
(7) Benmouna, M.; Weill, G.; Benoit, H.; Akcasu, A. Z. *J. Phys. (Orsay, Fr.)* **1982**, *43*, 1679.
(8) Koyama, R. *Physica B+C (Amsterdam)* **1983**, *120B*, 418.
(9) Pleštil, J.; Mikeš, J.; Dušek, K. *Acta Polym.* **1979**, *30*, 29.
(10) Ise, N.; et al. *J. Am. Chem. Soc.* **1979**, *101*, 5836; **1980**, *102*, 7901.
(11) Glatter, O.; Kratky, O. "Small-Angle X-ray Scattering"; Academic Press: London, 1982.
(12) Lifson, F.; Katchalsky, A. *J. Polym. Sci.* **1953**, *13*, 43.
(13) Katchalsky, A. *Pure Appl. Chem.* **1971**, *26*, 327.
(14) Oosawa, F. "Polyelectrolytes"; Marcel Dekker: New York, 1971.
(15) Manning, G. S. "Polyelectrolytes"; Sélégny, E., Mandel, M., Strauss, U. P., Eds.; D. Reidel: Dordrecht, 1974; p 9.
(16) Mandel, M. *Eur. Polym. J.* **1983**, *19*, 911.
(17) Fixman, M. *J. Chem. Phys.* **1979**, *70*, 4995.
(18) Manning, G. S. *Biophys. Chem.* **1977**, *7*, 95; **1978**, *9*, 65; *Q. Rev. Biophys.* **1978**, *11*, 179.
(19) Troll, M.; Zimm, B. H. *J. Phys. Chem.* **1983**, *87*, 3197.
(20) Kratky, O. "Instrumentation, Experimental Technique, Slit Collimation"; in ref 11, 1982; p 53.
(21) Stabinger, H.; Kratky, O. *Makromol. Chem.* **1978**, *179*, 1655.
(22) Urakawa, H.; et al., to be submitted.
(23) Akaike, H. *Proc. 5th Hawaii Int. Conf. Syst. Sci.* **1973**, 99.
(24) Glatter, O. *J. Appl. Crystallogr.* **1974**, *7*, 147.
(25) Guinier, A.; Fournet, G. "Small Angle Scattering of X-Rays"; translated by Walker, C. B.; Wiley: New York, 1955.
(26) de Gennes, P.-G. "Scaling Concepts in Polymer Physics"; Cornell University Press: Ithaca, NY, 1979.
(27) Yoon, D. Y.; Flory, P. J. *Macromolecules* **1976**, *9*, 249, 299.
(28) Kostorz, G. In "Treatise on Materials Science and Technology (Neutron Scattering)" Kostorz, G., Ed.; Academic Press: New York, 1979; Vol. 15 p 227.
(29) For example, see: "CRC Handbook of Chemistry and Physics" Weast, R. C., Ed.; CRC Press: Boca Raton, FL, 1981; p F-216.